

## The structure of disordered carbon solids studied using a hybrid reverse Monte Carlo algorithm

This article has been downloaded from IOPscience. Please scroll down to see the full text article.

2005 J. Phys.: Condens. Matter 17 2605

(<http://iopscience.iop.org/0953-8984/17/17/008>)

View [the table of contents for this issue](#), or go to the [journal homepage](#) for more

Download details:

IP Address: 129.252.86.83

The article was downloaded on 27/05/2010 at 20:40

Please note that [terms and conditions apply](#).

# The structure of disordered carbon solids studied using a hybrid reverse Monte Carlo algorithm

G Opletal, T C Petersen, D G McCulloch<sup>1</sup>, I K Snook and I Yarovsky

Applied Physics, School of Applied Sciences, RMIT University, GPO Box 2476V, Melbourne Vic. 3001, Australia

E-mail: dougal.mcculloch@rmit.edu.au

Received 14 December 2004, in final form 21 March 2005

Published 15 April 2005

Online at [stacks.iop.org/JPhysCM/17/2605](http://stacks.iop.org/JPhysCM/17/2605)

## Abstract

A hybrid reverse Monte Carlo (HRMC) algorithm, which incorporates both experimental and energy based constraints, is applied to investigate the microstructure of two disordered carbons of vastly different densities and bonding. We have developed a novel liquid quench procedure which in combination with the HRMC algorithm accurately describes the structure of these solids. Atomic networks generated by this approach are consistent with experimental and *ab initio* results and the method has been shown to overcome common difficulties associated with alternative approaches for modelling these complex systems. This procedure produces realistic large scale atomic structures which give a detailed picture of the structure of these solids.

## 1. Introduction

Accurate structural models of disordered solids are crucial for understanding the physical behaviour of existing materials and essential for many applications. Amorphous carbon (a-C) based solids are used in many industrial applications including coatings and as materials for filtration, purification and absorption based processes. For example, high density tetrahedral amorphous carbon (ta-C) coatings are important for tribological applications and porous carbon compounds are utilized in energy and steel production. Unfortunately, modelling the structures of these systems has proved difficult, mainly due to the configurational bonding flexibility of carbon, the lack of crystalline order and the presence of porosity.

A variety of films ranging from low density a-C to higher density ta-C can be produced using the condensation of energetic ions from plasmas [1–3]. The nature of the bonding and hence the microstructure within these films depends primarily upon the density. Diffraction studies provide averaged information about the structure in terms of the structure factor  $S(q)$  (where  $q$  is the magnitude of the scattering vector) and radial distribution function  $g(r)$  [4]

<sup>1</sup> Author to whom any correspondence should be addressed.

(where  $r$  is the interatomic pair separation) and many such experimental studies have been performed on disordered carbon solids [5, 6]. Unfortunately, direct analysis of diffraction data from disordered materials provides only limited structural information, because there is no direct relationship between such quantities as nearest neighbour distances and bond angle distributions, and the experimental data [7]. Simulation must therefore be used in conjunction with diffraction data to obtain detailed microstructural information for disordered systems.

In this work, we combine simulation with experimental diffraction data to investigate the structure of disordered carbon solids at densities of 2.4 and 3.0 g cm<sup>-3</sup>. These represent materials containing low and high fractions of atoms with diamond-like bonding, respectively. Moreover, accurate neutron diffraction data are available at these densities [8, 9].

Simulation of the deposition process effected by the arrival of individual ions is the most direct method for modelling the structure of deposited films [10–12]. Unfortunately, the very long simulation times limit the size of the systems that can be investigated. An alternative approach to modelling disordered structures is to simulate a ‘liquid quench’, in which a system is cooled very rapidly from a molten state to room temperature. It has been demonstrated by Marks [13] that structures resulting from ion bombardment techniques such as ion assisted deposition and using a filtered cathodic arc can be modelled accurately via such liquid quench simulations. Simulations of liquid quench systems are far less expensive than direct simulation of the deposition process, although surface information is lost since the method uses periodic boundary conditions (PBCs). The most sophisticated liquid quench simulations of a-C to date were performed by McCulloch *et al* [14] using the Car–Parrinello *ab initio* molecular dynamics (CPMD) method. However, their computationally intensive nature again limits the size of the system that can be simulated and rules out the estimation of uncertainties due to statistical fluctuations, which requires many separate simulations.

An alternative approach to modelling the structure of disordered materials is to use the reverse Monte Carlo (RMC) technique [15], which employs experimental scattering data. This technique has the advantage of generating three-dimensional atomic configurations consistent with these data and does not require simulation of the formation process or knowledge of the interatomic potential energy function. The main successful applications of the basic RMC method have been to systems which may be loosely described as ‘close packed’ structures such as liquid metals and disordered alloys. Unfortunately, in the case of disordered carbon solids, the conventional RMC algorithm produces highly unrealistic networks exemplified by a large population of small rings. These small rings are highly strained and therefore are unlikely to occur in large proportions in these solids.

In order to minimize the occurrence of very small, highly strained rings without introducing arbitrary assumptions about structure and bonding, we have developed a modified RMC algorithm which includes a constraint based on a many-body potential energy function, called the hybrid RMC (HRMC) method [16]. We have applied the HRMC method to successfully model low density systems dominated by sp<sup>2</sup> bonding such as glassy carbon [17]. In this work we have combined the HRMC algorithm with important modifications to the liquid quench approach to show that it is possible to describe the structure of a-C and ta-C which, by contrast, contains intermediate to high levels of sp<sup>3</sup> bonding.

## 2. Theoretical methods

The standard RMC algorithm uses a diffraction data constraint in which the difference between an experimental structure factor  $S(q)_{\text{EXP}}$  and that obtained from the simulation  $S(q)_{\text{RMC}}$  is minimized by use of a Markov process [15]. The assumption made is that the experimentally measured structure factor contains a normal distribution of statistical errors. The quantity to

be minimized,  $\chi^2$ , is given by

$$\chi^2 = \sum_{i=1}^N \frac{(S(q_i)_{\text{RMC}} - S(q_i)_{\text{EXP}})^2}{\sigma_{\text{EXP}}(q_i)^2} \quad (1)$$

where  $\sigma_{\text{EXP}}(q_i)$  is a measure of experimental uncertainty and  $N$  is the number of experimental data points. In addition, a similar  $g(r)$  constraint can also be added to the  $\chi^2$  function [18].

The conventional RMC method produces good fits to diffraction data with vastly different structures. For example, those involving unrealistically large proportions of highly strained three- and four-membered rings in covalently bonded systems. We have previously shown [17] that small ring acceptance is a simple, efficient but unphysical way of minimizing  $\chi^2$ . McGreevy *et al* [19] pointed out that, in general, the lack of uniqueness is due to a deficiency in the three-dimensional information contained in the ‘one-dimensional structure factor’. Thus diffraction data constraints alone are insufficient for modelling physically realistic structures.

In order to overcome these limitations, additional constraints can be applied to bond angles, ring statistics and coordination numbers. However, these require assumptions about the structure being modelled and therefore their application is limited. For example, O’Malley *et al* [7] modelled glassy carbon assuming a fully  $sp^2$  bonded network while Pikunic *et al* [20] modelled low density carbon using a bond angle constraint centred upon the graphitic bond angle peak and thus eliminating small rings. Unfortunately, such assumptions cannot be made for systems such as ta-C, which contain a mixture of atoms ranging in coordination and a non-trivial bond angle distribution. Another approach used by Walters *et al* [21] was to eliminate three-member rings via a ‘triplet’ constraint which rejected moves leading to their formation but this resulted in an unrealistically large four-member ring population.

Our HRMC algorithm [16] is a hybrid of the metropolis Monte Carlo (MMC) [22] method and the RMC method using an energy based constraint. The acceptance probability,  $P$ , in the HRMC algorithm is determined by equation (2):

$$P = e^{-\chi^2/2} e^{-\Delta E/kT} \quad (2)$$

where  $\Delta E$  is the change in energy due to the proposed Monte Carlo move and  $kT$  is the Boltzmann weighting factor. This potential reduces the occurrence of very unlikely, high energy configurations such as those produced by a large population of very small rings [16].

The purpose of the HRMC algorithm is to produce atomic configurations that are both consistent with experimental observations and are physically realistic. The nature of the structures produced and convergence of the algorithm depend upon the quality of the potential used. In this paper, we employed the environment dependent interaction potential (EDIP) [23], which has been shown to provide a good physical description of disordered carbon networks. To determine the appropriate weightings of the experimental and energetic constraints in equation (2), it is necessary to perform several simulations with the foremost aim being to achieve experimental consistency. Those calculations that result in the best EDIP energies are then chosen for statistical analysis through accumulation of atomic configurations throughout the final simulations.

### 3. Simulation systems and protocols

Table 1 summarizes the systems and simulation protocols used in this work. Simulations 1a, 1b and 1c were used to test the algorithms by comparing to previous *ab initio* CPMD simulations for the same system size [14]. Simulations 2 and 3 were used to assess the effect of increased system size at two different densities. Simulations 4 and 5 were performed to

**Table 1.** Details of the simulations performed. All systems used simple cubic initial configurations. MMC, RMC and HRMC refer to simulation protocols employed (see the text), while  $\sigma_{\text{EXP}}(q)$  is the measure of experimental uncertainty used in equation (1). Instant quenching involved changing the temperature over one Monte Carlo step. Slow quenching involved the temperature progression shown in figure 4. The  $\sigma(q)$  weighting factors were chosen to provide a balance between energy and experimental constraints.

Number	System		Schedule	Additional details
	Density	Number atoms		
1a	2.9	125	MMC, 5000 K equilibration, instantly quenched to 300 K, then run with RMC	$\sigma_{\text{EXP}}(q) = 0.03$
1b	2.9	125	MMC, 5000 K equilibration, instantly quenched to 300 K, then run with MMC	
1c	2.9	125	MMC, 5000 K equilibration, instantly quenched to 300 K, then run with HRMC	$\sigma_{\text{EXP}}(q) = 0.03$
2	3	24 389	MMC, 5000 K equilibration, instantly quenched to 300 K, then run with HRMC	$\sigma_{\text{EXP}}(q) = 0.01$
3	2.4	24 389	MMC, 5000 K equilibration, instantly quenched to 300 K, then run with HRMC	$\sigma_{\text{EXP}}(q) = 0.01$
4	3	2 197	HRMC mode, 5000 K equilibration, Slowly quenched to 300 K	$\sigma_{\text{EXP}}(q) = 0.01$
5	2.4	2 197	HRMC mode, 5000 K equilibration, Slowly quenched to 300 K	$\sigma_{\text{EXP}}(q) = 0.01$

provide detailed structural information using a refined liquid quench procedure combined with the most appropriate procedures identified by simulations 1–3.

## 4. Results and discussion

### 4.1. Evaluation of the HRMC method

In order to establish that large populations of small rings which plague conventional RMC simulations of disordered carbon can be overcome using the HRMC method, we performed liquid quench modelling of disordered carbon systems. Figure 1 shows the  $g(r)$ s produced from simulations 1a, 1b and 1c, in comparison with experiment [9]. As can be seen from the figure, the RMC (1a) and HRMC (1c) simulations produced very accurate fits; however the MMC (1b) simulation overestimated the first peak in  $g(r)$  by around 30%. Figure 2 shows the ring size distribution calculated using the shortest path criterion of Franzblau [24] for each simulation compared to that from CPMD [14]. Although the RMC method produced good agreement with the experimental data, the ring statistics show that the structure is dominated by unrealistic proportions of three-member rings. The MMC, HRMC and CPMD structures all have similar ring size distributions with variations which are typical for small systems.

In summary, it has been shown that HRMC produces ta-C structures that are more consistent with CPMD and more physically realistic than those produced by MMC and RMC

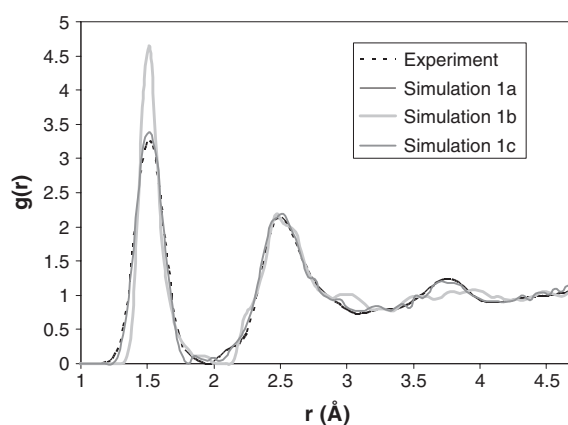


Figure 1.  $g(r)$  for simulations 1a, 1b, 1c (see table 1) compared to experiment [9].

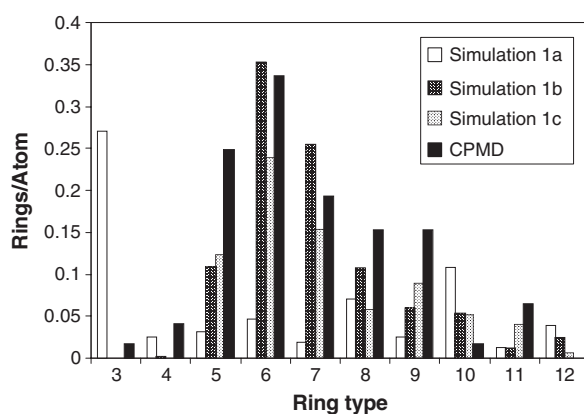
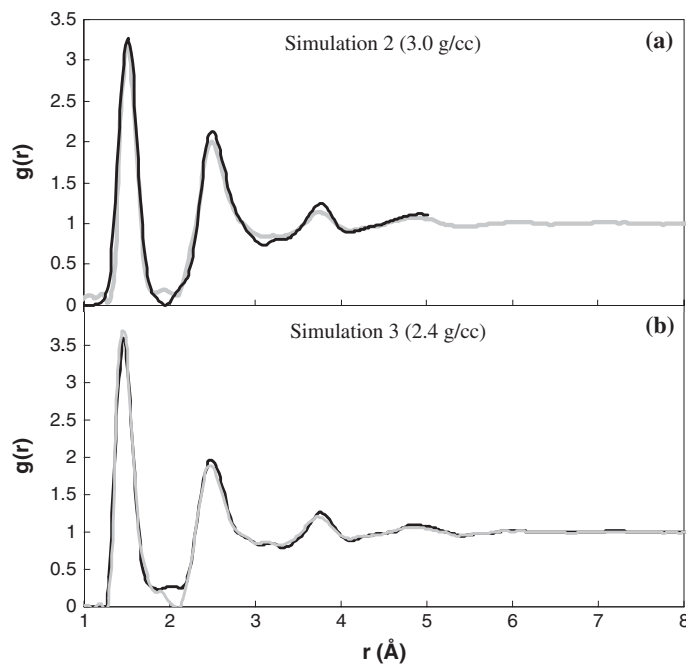


Figure 2. Ring size distribution for runs 1a, 1b, 1c (see table 1) compared to the *ab initio* CPMD simulations [14].

alone. However, these systems are not sufficiently large to enable accurate statistical data on some structural features particularly on the large scale to be obtained.

#### 4.2. Large system, instant quench simulations

In order to improve the statistics presented in the previous section, simulations were performed according to the method employed for simulation 1c, using a larger number of particles for both  $2.4$  and  $3.0 \text{ g cm}^{-3}$  systems (runs 2 and 3 in table 1). Figures 3(a) and (b) show the  $g(r)$ s for simulations 2 and 3 compared with experimental neutron data. Both  $g(r)$ s present some discrepancies between the first and second peaks. There is a shoulder on the first peak in the  $g(r)$  for simulation 2, which indicates the presence of locally strained structures characteristic of the instant quench procedure for the MMC generated liquid phase. Besides increasing the number of atoms for improved statistics, this result suggests a more gradual quench procedure performed with HRMC is required to allow the system to rearrange to structures more characteristic of the solid.



**Figure 3.** (a)  $g(r)$  comparison between simulation 2 (grey line) and experimental neutron scattering data [9] (black line). (b)  $g(r)$  comparison between simulation 3 (grey line) and experimental neutron scattering data [8] (black line).

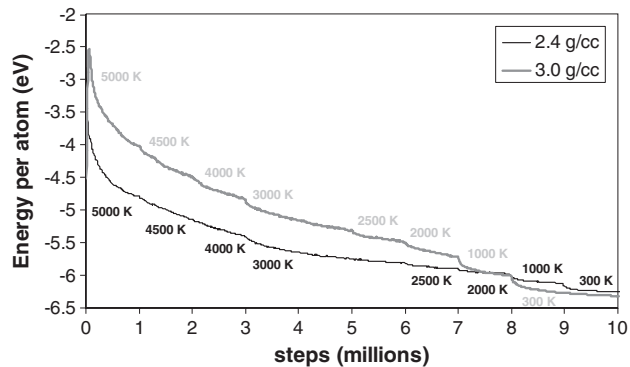


**Figure 4.** The energy per atom of the quench scheme in HRMC mode for simulations 4 and 5. Also shown is the temperature progression for each simulation.

#### 4.3. Medium system, slow quench simulations

In this section, we present a gradual quench procedure, designed to overcome the remaining effects of unrealistic bonding configurations described in the previous section. The method employs all constraints (HRMC mode) throughout the entire simulation but varies the temperature  $T$  throughout the quench procedure. Figure 4 shows the energy and temperature evolution during the quench procedure throughout simulations 4 and 5 and it can be seen that, as the temperature is decreased, both systems smoothly drop in energy and equilibrate to 300 K.

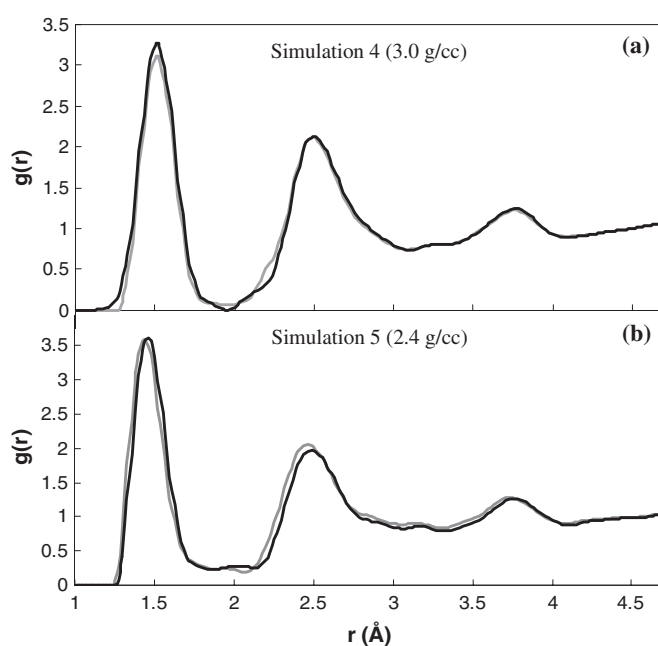


**Figure 5.** (a)  $g(r)$  comparison between simulation 4 (grey line) system and experimental neutron scattering data [9] (black line). (b)  $g(r)$  comparison between simulation 4 (grey line) system and experimental neutron scattering data [8] (black line).

The  $g(r)$  and  $S(q)$  for these systems are shown in figures 5 and 6 respectively. Agreement with experimental data is now very good at both densities, except for the low  $q$  region for the experimental  $S(q)$ , where the experimental data are difficult to obtain accurately. Furthermore, some of the deviation at low  $Q$  could be due to the finite size of the model used. Thus it is clear that the new quenching procedure successfully models the experimental data whilst simultaneously producing low energy structures.

## 5. Analysis of the disordered carbon solid structures

The ring statistics for simulations 4 and 5 are shown in figure 7 and indicate overall similar ring distributions for the two densities. It can be seen that the dominant rings size is 6, whilst there are more small rings in the higher density system. It should be noted that the low percentage of small rings is consistent with CPMD simulations.

Figure 8 compares the coordination distributions for the two systems, calculated using a coordination sphere of radius 1.85 Å. It is evident that the low density system is dominated by threefold-coordinated atoms, with a significant presence of twofold- and fourfold-coordinated atoms. By contrast, the higher density network exhibits three- and four-coordinated atoms in approximately equal proportions.

Coordination resolved bond angle distributions shown in figures 9(a) and (b) reveal more subtle differences between the two structures. First, for the high density system a small peak at approximately  $60^\circ$  is observed, which is characteristic of the three-membered rings. There is also a shoulder at  $90^\circ$  in the  $3.0 \text{ g cm}^{-3}$  system, associated with four-membered rings. In both systems, it is seen that the bond angles correlate with the coordination types, with threefold-coordinated atoms centred about  $118^\circ$ , indicative of a graphitic microstructure.



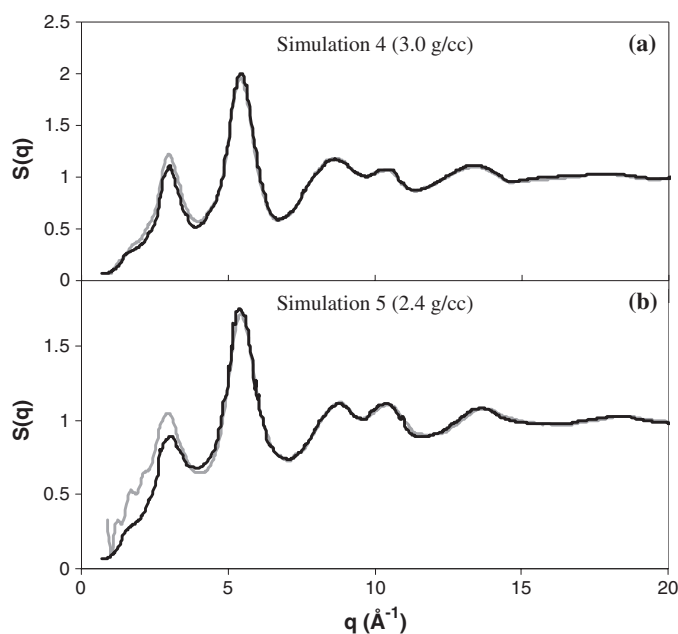


**Figure 6.** (a)  $S(q)$  comparison between simulation 4 (grey line) system and experimental neutron scattering data [9] (black line). (b)  $S(q)$  comparison between simulation 4 (grey line) system and experimental neutron scattering data [8] (black line).

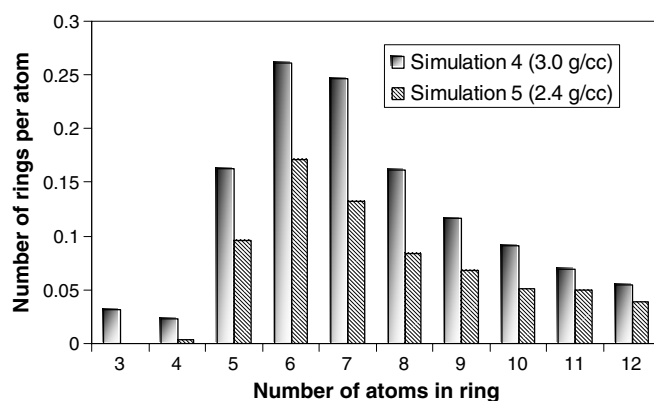


**Figure 7.** Ring size distributions for simulations 4 and 5.

Likewise, the fourfold-coordinated atoms are centred about  $112^\circ$ , close to the tetrahedral bonding arrangement of diamond.

In order to provide a qualitative picture of the quantitative data shown in the graphs, we include figures 10 and 11, which show representative atomic configurations for simulations 4 and 5 respectively. These figures highlight the main differences between the total network structures for each density. The domination of threefold-coordinated atoms (light grey) in the low density network is evident, with other coordinated atoms interspersed throughout. By contrast, the high density network is shown to contain approximately equal proportions of both three- and four-coordinated atoms.

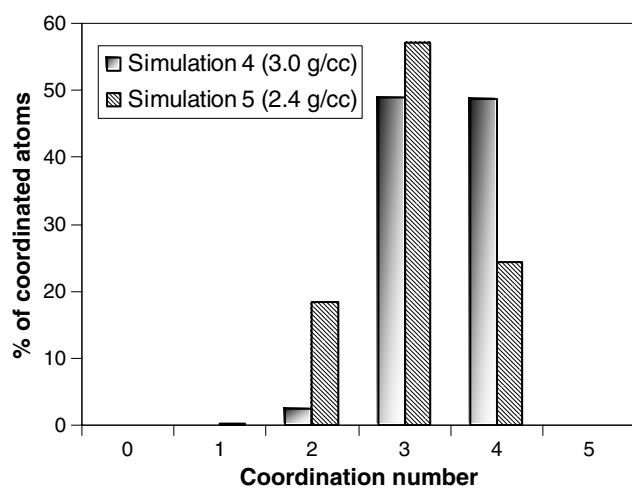


Figure 8. Coordination distributions for simulations 4 and 5.

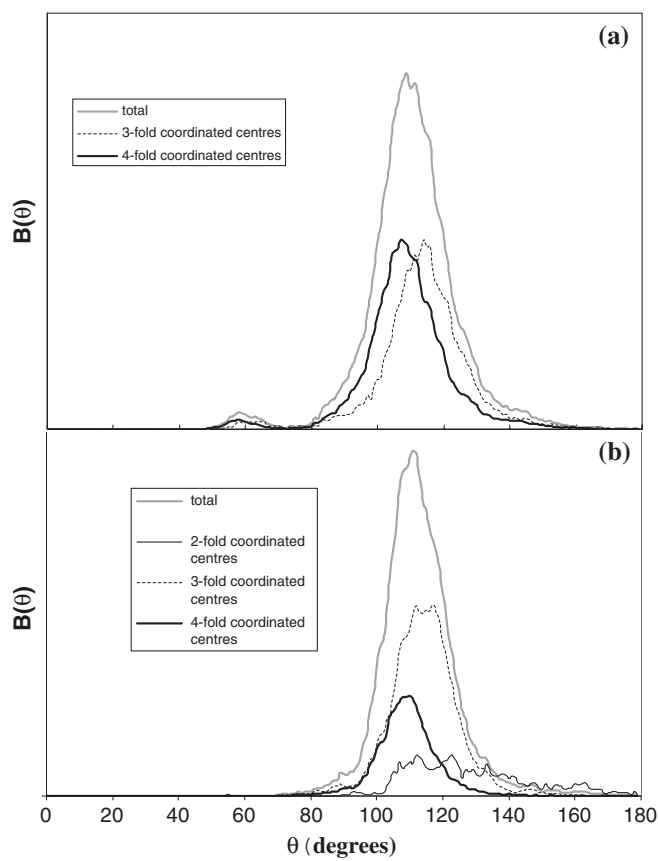
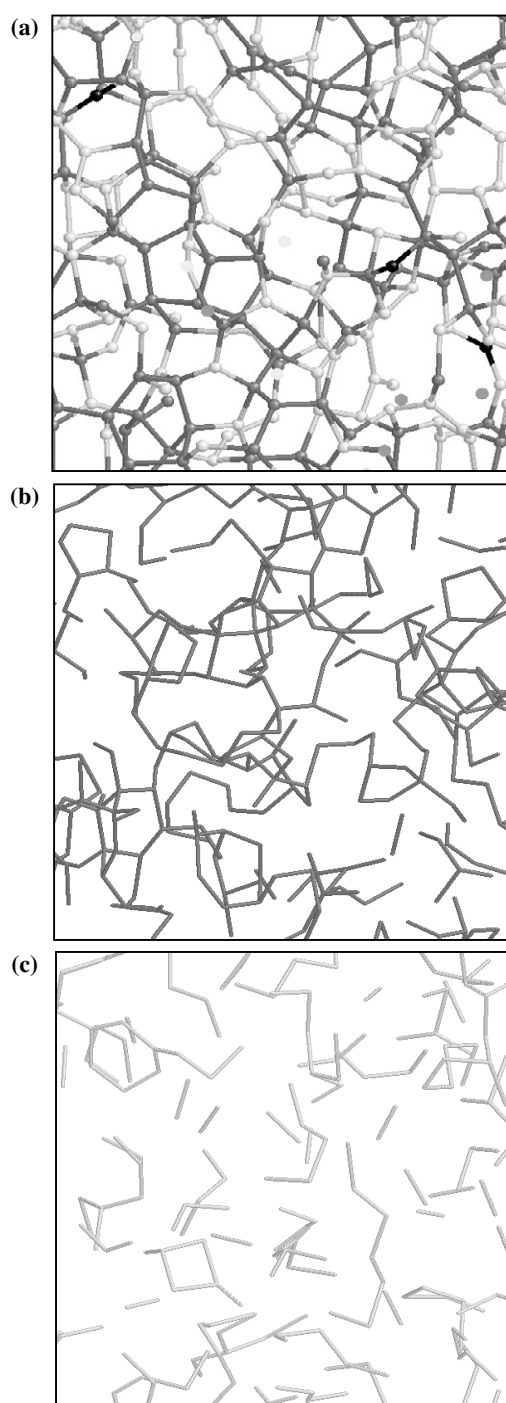
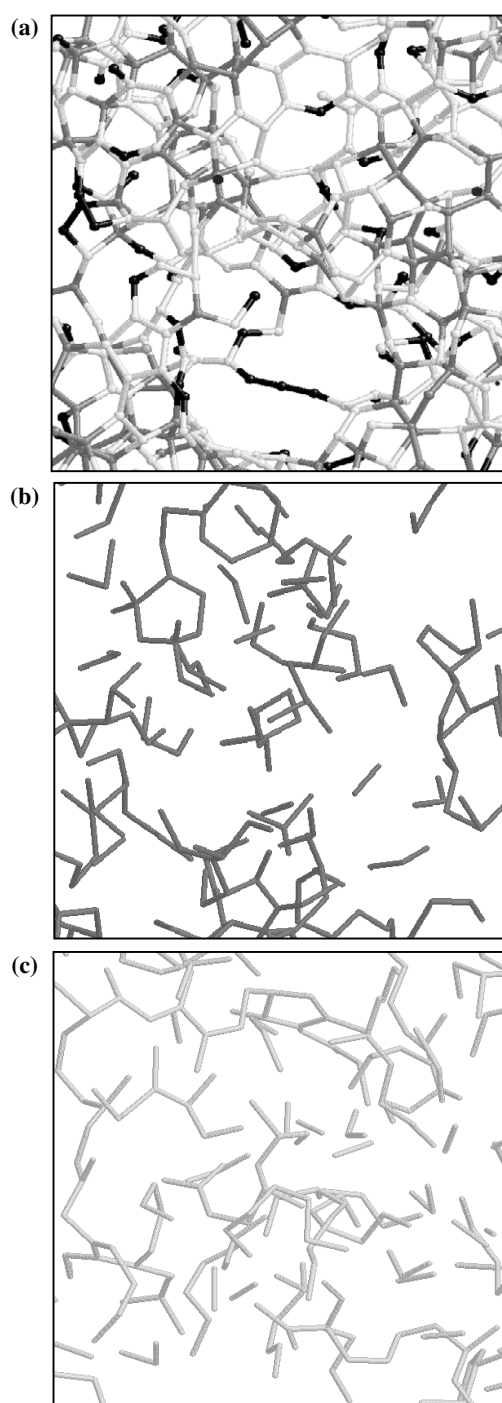


Figure 9. (a) Threefold- and fourfold-coordination contributions to the average bond angle distribution for simulation 4 (3.0 g cm<sup>-3</sup> system). (b) Twofold-, threefold- and fourfold-coordination contributions to the average bond angle distribution for simulation 5 (2.4 g cm<sup>-3</sup> system).



**Figure 10.** (a) Narrow section of a typical atomic configuration from simulation 4 ( $3.0 \text{ g cm}^{-3}$  system). Black, light grey and dark grey bonds refer to twofold-, threefold- and fourfold-coordinated atoms respectively. In (b) and (c) bond specific views are shown for fourfold to fourfold and threefold to threefold bonding respectively.



**Figure 11.** (a) Narrow section of a typical atomic configuration from simulation 5 ( $2.4 \text{ g cm}^{-3}$  system). Black, light grey and dark grey bonds refer to twofold-, threefold- and fourfold-coordinated atoms respectively. In (b) and (c) bond specific views are shown for fourfold to fourfold and threefold to threefold bonding respectively.

## 6. Conclusion

We have demonstrated that the HRMC algorithm, combined with a modified liquid quench procedure, is capable of describing the experimental structural data for disordered carbon at both low and high densities. Structures generated by this approach are consistent with experimental and *ab initio* results. We have also established that RMC modelling alone does not generate realistic networks for these systems, whilst the MMC method alone produces feasible structures that however do not conform to experiment. This has enabled the production of detailed atomic structures on larger scales than is possible using *ab initio* simulations. These structures are required to describe interesting large scale features such as nanoporosity and large scale defects. Such work is currently under way.

## Acknowledgments

The Victorian Partnership for Advanced Computing (VPAC) provided computer time for performing the HRMC simulations. The authors would like to thank Dr Nigel Marks of the Department of Applied Physics, School of Physics (A28), University of Sydney, NSW 2006, Australia, for allowing the use of his carbon EDIP. Furthermore, the authors would like to thank Dr Brendan O'Malley, Unilever R&D Port Sunlight, Bebington, Wirral, UK, for allowing the use of his ring statistics codes and his significant involvement with the development of the simulation code.

## References

- [1] Fallon P J, Veerasamy V S, Davis C A, Robertson J, Amaratunga G A J, Milne W I and Koskinen J 1993 *Phys. Rev. B* **48** 4777
- [2] Schwan J, Ulrich S, Theel T, Roth H, Ehrhardt H, Becker P and Silva S R P 1997 *J. Appl. Phys.* **82** 6024
- [3] McKenzie D R, Muller D and Pailthorpe B A 1991 *Phys. Rev. Lett.* **67** 773
- [4] Warren B E 1969 *X-ray Diffraction* (Reading, MA: Addison-Wesley)
- [5] Etherington G, Wright A C, Wenzel J T, Dore J C, Clarke J H and Sinclair R N 1982 *J. Non-Cryst. Solids* **48** 265
- [6] Gaskell P H, Saeed A, Chieux P and McKenzie D R 1991 *Phys. Rev. Lett.* **67** 1286
- [7] O'Malley B, Snook I and McCulloch D G 1998 *Phys. Rev. B* **57** 14148
- [8] Li F and Lannin J S 1990 *Phys. Rev. Lett.* **65** 1905
- [9] Gilkes K W R, Gaskell P H and Robertson J 1995 *Phys. Rev. B* **51** 12303
- [10] Kaukonen H P and Nieminen R M 1992 *Phys. Rev. Lett.* **68** 620
- [11] Jäger H U and Albe K 2000 *J. Appl. Phys.* **88** 1129
- [12] Uhlmann S, Frauenheim Th and Lifshitz Y 1998 *Phys. Rev. Lett.* **81** 641
- [13] Marks N A 1997 *Phys. Rev. B* **56** 2441
- [14] McCulloch D G, McKenzie D R and Goringe C M 2000 *Phys. Rev. B* **61** 2349
- [15] McGreevy R L and Pusztai L 1988 *Mol. Simul.* **1** 359
- [16] Opletal G, Petersen T, O'Malley B, Snook I, McCulloch D G, Marks N A and Yarovsky I 2002 *Mol. Simul.* **28** 927
- [17] Petersen T, Yarovsky I, Snook I, McCulloch D G and Opletal G 2003 *Carbon* **41** 2403
- [18] Toth G and Baranyai A 1999 *Mol. Phys.* **97** 339
- [19] McGreevy R L, Howe M A, Keen D A and Clausen K N 1990 *Inst. Phys. Conf. Ser.* **107** 165
- [20] Pikunic J, Pellenq R J M, Thomson K T, Rouzaud J N, Levitz P and Gubbins K E 2001 *Stud. Surf. Sci. Catal.* **132** 647
- [21] Walters J K, Gilkes K R, Wicks J D and Newport R J 1998 *Phys. Rev. B* **58** 8267
- [22] Metropolis N, Rosenbluth A W, Rosenbluth M N, Teller A H and Teller E 1953 *J. Chem. Phys.* **21** 1087
- [23] Marks N A 2001 *Phys. Rev. B* **63** 03540
- [24] Franzblau D S 1991 *Phys. Rev. B* **44** 4925